

JAERI - M  
89-149

TRANSPORT MODELLING BY A HEAT PINCH  
THEORY IN THE JT-60 TOKAMAK

October 1989

Mitsuru KIKUCHI and Masafumi AZUMI

日本原子力研究所  
Japan Atomic Energy Research Institute

JAERI-M レポートは、日本原子力研究所が不定期に公刊している研究報告書です。  
入手の間合わせは、日本原子力研究所技術情報部情報資料課（〒319-11 茨城県那珂郡東海村）  
あて、お申しこしください。なお、このほかに財団法人原子力弘済会資料センター（〒319-11 茨城  
県那珂郡東海村日本原子力研究所内）で複写による実費頒布をおこなっております。

JAERI-M reports are issued irregularly.  
Inquiries about availability of the reports should be addressed to Information Division, Department  
of Technical Information, Japan Atomic Energy Research Institute, Tokai-mura, Naka-gun,  
Ibaraki-ken 319-11, Japan.

© Japan Atomic Energy Research Institute, 1989

---

編集兼発行 日本原子力研究所  
印刷 山田軽印刷所

Transport Modelling by a Heat Pinch Theory  
in the JT-60 Tokamak

Mitsuru KIKUCHI and Masafumi AZUMI

Department of Large Tokamak Research  
Naka Fusion Research Establishment  
Japan Atomic Energy Research Institute  
Naka-machi, Naka-gun, Ibaraki-ken

(Received September 19, 1989)

Energy confinement properties of the JT-60 tokamak during the ohmic and neutral beam heated discharges are analyzed based on the heat pinch model proposed by Callen and Cordey. The temperature profile consistency against the density profile variation sets an important constraint for the heat pinch term. The heat pinch proportional to  $n_e B_p$  seems to be consistent with the experimental observation. The model reproduces the parameter dependences of JT-60 experimental data quite well. The formation of the edge temperature pedestal during the H-mode is naturally observed with this model when the edge convective energy loss is significantly reduced.

Keywords: Heat Pinch, Profile Consistency, Energy Confinement,  
Offset-linear Scaling, JT-60

熱ピンチ理論による JT-60 トカマクのエネルギー輸送モデル

日本原子力研究所那珂研究所臨界プラズマ研究部

菊池 満・安積 正史

(1989年9月19日受理)

JT-60 トカマクのジュール加熱及びNBI加熱プラズマのエネルギー閉じ込め特性を、Callen と Cordey によって提案された熱ピンチモデルに基づいて解析した。密度分布の変化に対する温度分布不変性は熱ピンチに対して重要な制約条件を課す。 $n_e B_p$  に比例する熱ピンチが実験結果と一致するように思われる。このモデルは JT-60 の実験データのパラメータ依存性を良好に再現する。Hモード中の周辺部  $T_e$ 、ペDESTAL形成も、周辺部の対流損失が小さいときに、このモデルで自然に生じる。

Contents

1. Introduction .....	1
2. Transport Modelling based on the Heat Pinch .....	2
3. Formation of the Edge Transport Barrier in the H-mode .....	9
4. Discussion and Conclusion .....	10
Acknowledgements .....	10
References .....	11

目 次

1. はじめに .....	1
2. 熱ピンチに基づく輸送モデル .....	2
3. Hモードにおける周辺輸送バリアの形成 .....	9
4. 考察・結論 .....	10
謝 辞 .....	10
参考文献 .....	11

## 1. INTRODUCTION

Understanding of the energy confinement properties of a tokamak with relatively simple confinement model is not successful up to now. However there are many important experimental observations concerning the confinement properties in a tokamak, the temperature profile consistency ( or resilience ), good energy confinement in ohmic plasma with fairly high thermal conduction coefficient measured by the heat pulse propagation technique compared with those from the profile analysis, a low incremental energy confinement time during the auxiliary heating in contrast to the ohmic heating case. In this paper, efforts are made to develop a heat transport model based on the heat pinch proposed by Callen and Cordey [1,2].

The heat pulse propagation study in the TFTR tokamak [3] shows a large difference in the electron thermal conduction coefficients obtained from the heat pulse propagation and those from the power balance analysis. They discussed the origin of such a large difference including the heat pinch suggested by R.J. Hawryluk. The JET tokamak also exhibits such an enhancement of the electron heat transport during the heat pulse propagation study in both ohmic and auxiliary heated discharges[4]. They also found that the electron thermal conductivity measured by the heat pulse propagation  $\chi_e^{HP}$  is independent of the power and agrees with the incremental electron thermal conductivity calculated from the power balance analysis. Callen [1] proposed a transport model which is consistent with the temperature profile resilience, the enhanced electron thermal conduction coefficient and the global energy confinement in the JET tokamak. He also introduced the heating effectiveness and showed that the model agrees with the localized off-axis ICRF heating results. But he did not discuss the density dependence of the heat pinch. Goldston pointed out the importance of the density dependence in the heat pinch analysis [5]. We have shown that the importance of the density dependence to study the offset linear scaling[6]. The ohmic stored energy which represents the strength of the heat pinch increases strongly with the plasma density and the plasma current. Here we will develop a heat pinch model consistent with such observations. The heat pinch and the thermal conduction coefficient consistent with JT-60 energy confinement are given in the following section. The formation of the edge temperature pedestal during the H mode is discussed in relation to the model in section 3. The discussions and conclusions are given in section 4.

## 2. TRANSPORT MODELLING BASED ON THE HEAT PINCH

The purpose of this section is to develop the plasma confinement model based on the heat pinch with particular attention on the role of the plasma density. As is shown in our paper [6], the plasma stored energy during the ohmic heating increases with the average plasma density. The incremental energy confinement time for the thermal component is independent (or weakly dependent) of the plasma density and the plasma current although the current scan is not fully made. Figure 1 illustrates the offset linear relations as a function of the plasma density. Figure 1a shows the 3-dimensional plot of the plasma stored energy as a function of the  $n_e$  and  $P_{abs}$ . The ohmic stored energy increases with plasma density and the extrapolated heat pinch increases with plasma density. Figure 1b shows the offset linear relations for low and high density cases. The offset stored energy is small for the low density case and large in high density case which suggests the heat pinch increases with plasma density.

Let us start with the following energy balance equation,

$$-\frac{1}{r} \frac{d}{dr} (rn\chi \frac{dT}{dr}) + \frac{1}{r} \frac{d}{dr} (\frac{5}{2} nTv) = P_h - P_R \quad (1)$$

where,  $n$ ,  $T$ ,  $v$ ,  $P_h$  and  $P_R$  are density, temperature, radial flow velocity, heating power density and the radiation power density, respectively. The volume integral of the equation (1) gives the energy flow balance across the magnetic surface as follows,

$$S(r) [-n(r)\chi(r) \frac{dT}{dr} + \frac{5}{2} nTv] = Q_h \quad (2)$$

$$S(r) = 4\pi^2 R_p r$$

$$Q_h = \int_0^r P_h dV(r)$$

where  $S$  and  $Q_h$  are the surface area and the heating power inside the magnetic surface, respectively. Here, the radiation loss is neglected for simplicity. The heat pinch model [1] assumes that the total heat flux is given by,

$$q = -n\chi \frac{dT}{dr} = -n\chi_{inc} \frac{dT}{dr} - q_{in} \quad (3)$$

where  $\chi_{inc}$  and  $q_{in}$  are the incremental  $\chi$  and the non diffusive heat flow (inward heat pinch), respectively. Based on the experimental agreement of the  $\chi_e$  measured by the heat pulse propagation with the  $\chi_e^{inc}$  evaluated from the power balance analysis, Callen and the JET team proposed the heat pinch model with constant  $\chi_{inc}$  and  $q_{in}$ . Such an offset

linear relation of the heat conduction is also confirmed in JT-60 by the power balance study as shown in Fig.2. But the density dependence of such quantities are not clear from their results. The incremental thermal conductivity  $\chi_{inc}$  is independent of the average density as is clear from our result [6] in which the energy loss is shown to be dominated by the conduction loss and the incremental energy confinement time for the thermal component is independent of the density. On the other hand, the heat pinch flux must increase with the plasma density.

The power balance equation (2) is written for the ohmic heating case as follows,

$$-n(r)\chi_{inc}(r)\frac{dT}{dr} - q_{in} + \frac{5}{2}nTv = q_{OH} = \frac{E_z B_p}{\mu_0} \quad (4)$$

where the right hand side represents the Poynting energy flux. If we neglect the convective energy loss term which is important near the plasma edge, the temperature profile is given by,

$$T(r) = \int_r^a \frac{q_{in} + q_{OH}}{n\chi_{inc}} dr \quad (5)$$

One of important characteristics of the temperature profile is the profile resilience against the density profile variation. We usually observe a peaked density profile for the limiter configuration and a flat density profile for the outside divertor configuration in JT-60. Figure 3 shows the temperature and density profiles for the limiter and divertor discharges for ohmic and neutral beam heated discharges. As is clear from the figure, the temperature profile does not change when the density profile is changed. For the classical transport modelling  $q_{in} = q_{in}^{NC}$  with INTOR/ALCATOR scaling  $\chi_e \sim 1/n_e$ ,  $\kappa_e = n_e \chi_e$  is uniform and the temperature profile shape is kept constant even if the density profile is changed. For the constant  $\chi_{inc}$  and  $q_{in}$  model used in [1], the temperature profile consistency will break in response to the density profile variation. Therefore in order to keep the profile consistency against the density profile variation, the heat pinch term  $q_{in}$  ( $\gg q_{OH}$ ) directly proportional to the local plasma density is desirable to cancel the density term in the denominator. Moreover, the heat pinch term proportional to the density seems to reproduce the experimental  $\bar{n}_e$  dependence of the plasma stored energy. The plasma stored energy  $W_s$  was well expressed by the following expression in JT-60 ohmic discharges [6].

$$w_s(\text{MJ}) = 0.157 I_p^{0.86} (\text{MA}) \bar{n}_e^{0.62} (10^{19} \text{m}^{-3}) \quad (6)$$



The plasma stored energy increases with increasing plasma current and density. The experimental ohmic stored energy is shown as a function of the  $\bar{n}_e$  in Fig.4. The plasma stored energy expected from the heat pinch model is given by,

$$W_s = \int_0^a dr S(r) 3n(r) T(r) \quad (7)$$

$$= \int_0^a dr S(r) 3n(r) \int_r^a \frac{[q_{in} + q_{OH}]}{n \chi_{inc}} dr' \quad (8)$$

Taking account of the weak ( almost none )  $I_p$  and  $n_e$  dependences of the incremental energy confinement time during the L-mode discharge [6,7],  $\chi_{inc}$  must be independent of  $I_p$  and  $n_e$ [4] because the dominant loss is not the convection loss but the conduction loss except near the very edge. The following form of the heat pinch  $q_{in}$  can reproduce the experimental ohmic stored energy taking account of  $q_{in} \gg q_{OH}$ ,

$$q_{in} = K r B_p(r) n_e(r) \quad (9)$$

where K is a numerical constant. Here an arbitrariness of the radial profile may exist. The neoclassical transport theory predicts an inward heat pinch ( associated with the Ware pinch ) which is given as follows [8],

$$q_{in} = K_{23} n_e(r) T_e(r) \sqrt{E} \frac{E_z(r)}{B_p(r)} \quad (10)$$

But the absolute value and the parameter dependences are quite different between these formulas.

In order to determine the radial profile of  $\chi_{inc}$ , the temperature profile peakedness  $\gamma_T$  measured with the Thomson scattering system is plotted as a function of  $1/q_{eff}$  in Fig.5 together with the radius of the  $q = 1$  surface evaluated from the sawtooth inversion radius. The best fit of the temperature peakedness  $\gamma_T$  is given by,

$$\gamma_T = \frac{T_e(0)}{\langle T_e \rangle} = 1.0 + 0.5q_{\text{eff}}^{2/3} \quad (11)$$

So the following form of the temperature profile seems to be a good description of the experimental observation,

$$T_e(r) = T_e(0)(1-(r/a)^2)^{0.5q_{\text{eff}}^{2/3}} \quad (12)$$

The current profile can be calculated with the neoclassical resistivity. Here, we use the most simple expression for the current profile in the collisionless limit as follows,

$$J(r) = J_0 \left( \frac{T_e(r)}{T_e(0)} \right)^{1.5} f_c(r) \quad (13)$$

where  $f_c$  is the fraction of the circulating electrons which primarily contribute the plasma current as follows,

$$f_c = \frac{(1-\epsilon)^2}{\sqrt{1-\epsilon^2}} \frac{1}{1+1.46\sqrt{\epsilon}} \quad (14)$$

The radius of the  $q = 1$  surface calculated with this  $J(r)$  profile agrees with the experimental observation as shown by the solid line in Fig.5(b). The calculated temperature, current and safety factor profiles are shown in Fig.6. This result is consistent with our experimental investigation of the neoclassical resistivity [9]. In order to match the experimental temperature profile, following form of  $\chi_{\text{inc}}$  is desirable.

$$\chi_{\text{inc}} = \frac{2\chi_0}{q_{\text{eff}}^{2/3}(1-(r/a)^2)^{0.5q_{\text{eff}}^{2/3}-1}} \quad (15)$$

Here it should be noted that the equation (15) is not a single expression and apparently the  $\chi_{\text{inc}}$  expression using the local physical quantities such as the shear and the safety factor is favorable. Also  $\chi_{\text{inc}}$  near the edge is not correct due to the neglect of the convective energy loss. Then the remaining subjects are to get the numerical constants  $\chi_0$

and K. In order to get these constants, we proceed to the case of the auxiliary heating discharges.

The plasma stored energy during the auxiliary heating is given by the following form [1],

$$W_p = 3 \int_0^a n T dV = W_{\text{pinch}} + W_{\text{inc}} \quad (16)$$

where ,

$$W_{\text{pinch}} = \int_0^a \frac{3N(r)q_{\text{in}}(r)}{n(r)\chi_{\text{inc}}(r)} dr \quad (17)$$

$$\begin{aligned} W_{\text{inc}} &= \int_0^a \frac{3N(r)q_h(r)}{n(r)\chi_{\text{inc}}(r)} dr \\ &= \tau_\chi \int_0^a P_h(r)(1-y(r)) dr \end{aligned} \quad (18)$$

$$N(r) = \int_0^r n(r') dV(r') \quad q_h = \frac{Q_h}{S(r)} \quad (19)$$

$$\tau_\chi = \frac{3}{4\pi^2 R_p} \int_0^a \frac{N(r) dr}{n(r)\chi_{\text{inc}}(r)} \quad (20)$$

$$y(r) = \frac{\int_0^r \frac{N(r') dr'}{n(r')\chi_{\text{inc}}(r')}}{\int_0^a \frac{N(r') dr'}{n(r')\chi_{\text{inc}}(r')}} \quad (21)$$

The plasma stored energy can be rewritten with the introduction of the heating effectiveness as follows,

$$W_s = W_{\text{pinch}} + \tau_E^{\text{inc}} P_{\text{abs}} \quad (22)$$

$$\tau_E^{\text{inc}} = \eta_h \eta_{\text{cx}} \tau_\chi \quad (23)$$

$$\eta_h = \frac{\int_0^a P_h(r)(1-y(r))dr}{\int_0^a P_h(r)dr} \quad (24)$$

where  $\eta_h$  and  $\eta_{cx}$  are the heating effectiveness and the power reduction fraction of the absorbed beam power due to the charge exchange loss of the fast ions, respectively. The  $\eta_{cx}$  is in the range of 0.95-0.8 depending on the particle confinement time and the density. The density profile in the outside divertor is almost flat in high density regime as shown in Fig.4. In such cases, the ideal incremental confinement time  $\tau_\chi$  is given as follows,

$$\tau_\chi = \frac{3a^2}{4\chi_0} \quad (25)$$

Assuming the following heating profile,

$$P_h = P_{h0}(1-(r/a)^2)^{\alpha_h} \quad (\alpha_h = 0.3-2) \quad (26)$$

the heating effectiveness  $\eta_h$  is analytically given by,

$$\eta_h = \frac{1+\alpha_h}{1+\alpha_h+0.5q_{\text{eff}}^{2/3}} \quad (27)$$

In order to explain the experimental  $\tau_E^{\text{inc}}$  of 60 m sec, we have

$$\chi_0 = 7 \text{ m}^2/\text{sec} \quad (28)$$

The numerical constant K is determined from the experimental ohmic stored energy as  $K = 6 \times 10^{-15} \text{ W/T}$ .

With these preparations of the transport modelling, we can check our model with the experimental results. Here, it should be noted that the derivation procedure of the transport coefficients is not logical at all. The transport coefficients proposed above could be a candidate only when the predicted confinement properties is consistent with the experimental observations.

Let us start with the ohmic confinement properties of JT-60. The plasma stored energy  $W_s$  and the temperature peakedness parameter  $\Upsilon_T = \frac{T_e(0)}{\langle T_e \rangle}$  calculated using the equations (5) and (8) are plotted as a function of the line averaged electron density  $\bar{n}_e$  in Fig.7 together

with the experimental plasma stored energy[ 6]. The model reproduces the experimental plasma stored energy quite well. Here the density profile is assumed as,

$$\begin{aligned} n_e &= n_{e0} \left(1 - \left(\frac{r}{a}\right)^2\right)^{\alpha_n} \\ \alpha_n &= 1.2 + 0.5/\bar{n}_e \end{aligned} \quad (29)$$

Radial profiles of the assumed heat pinch and the Poynting energy flux are shown in Fig.8 for low and high density cases. As is clear from the figure, the heat pinch  $q_{in}$  is higher than the ohmic Poynting energy flux  $q_{OH}$ . One of important characteristics is the heat pinch and Poynting energy fluxes near the plasma surface. The heat pinch must be a heat flux caused by the internal plasma dynamics if it exists. Therefore the heat pinch flux at the plasma surface must be zero because no energy flux is supplied from outside of the plasma surface where no plasma exists. On the other hand, the Poynting energy flux is the real external energy flux supplied from outside of the plasma. Therefore the heat flux  $S(r)q_{in}$  must be maximum and non-zero at the plasma surface. Assumed heat pinch term satisfies the above physical requirement similar to the neoclassical heat pinch.

Secondly, we have compared the model with the auxiliary heating case. Figure 9 shows the kinetic stored energy calculated from the model compared with the measurement for the 2MA power scan. The agreement between our model and the experimental result is fairly good. The radial profile of the heat pinch and the heat fluxes by the NBI heating is shown in Fig.10. The same characteristics of the  $q_{in}$  and  $q_h$  discussed in the ohmic heating case are seen in the figure. The temperature profile peakedness parameter  $\Upsilon_T$  is calculated for various heating profiles as shown in Fig.11. The temperature profile resilience holds for our model in response to the heating profile. An important consequence from our model is the break-down of the profile consistency in very low density regime because the heat pinch is extremely small in such a regime. This is consistent with the experimental observation of an extremely peaked temperature profile during the LHCD experiments [10].

The effectiveness of the transport model described above is checked using the 1.5D transport code [11] in which neutral transport, beam deposition, impurity effect and electron-ion energy transport are included. Figure 12 shows the power and density scans for 2MA discharges. The heat pinch terms, thermal conduction coefficients for electrons and ions and the particle confinement time at the plasma surface are assumed as follows,

$$q_{in}(e) = q_{in}(i) = Kr n_e B_p, \quad K = 6 \times 10^{-15} \text{W/T}$$

$$\begin{aligned}\chi_e^{\text{inc}} &= \chi_i^{\text{inc}} = 5 \text{ m}^2/\text{sec} \text{ (uniform)} \\ \tau_p &= 40 \text{ msec} , \sigma = \sigma^{\text{NC}} , Z_{\text{eff}} = 1.0 \\ \bar{n}_e &= 4 \times 10^{19} \text{ m}^{-3} , \text{ multi-pencil beam+Stix solution.}\end{aligned}$$

The agreement with the experimental results is fairly good.

### 3. FORMATION OF THE EDGE TRANSPORT BARRIER IN THE H-MODE

The formation of the edge transport barrier is the most important characteristics of the H mode [12]. The formation of the edge pedestal is associated with the improvement in the particle confinement at the plasma edge which reduces the convective energy loss near the plasma surface [13]. The temperature gradient in our model without the edge convective loss is given by,

$$\frac{dT(r)}{dr} = - \frac{q_{\text{in}} + q_{\text{h}}}{n_e \chi_{\text{inc}}} \quad (30)$$

where,  $q_{\text{h}} = Q_{\text{h}}/S(r)$  is the external heating flux. If the  $\chi_{\text{inc}}$  is finite at the plasma edge, the denominator in the right hand side of the equation (30) becomes zero at the plasma surface. Although  $q_{\text{in}}$  is also zero at the plasma surface,  $q_{\text{h}}$  is finite at the plasma surface. Therefore the temperature gradient at the plasma edge can be very large during a high power heating when the particle confinement is sufficiently good. The formation of the steep temperature gradient at the plasma edge depends strongly on the edge plasma density. For sufficiently low edge plasma density, a steep temperature gradient can be formed. The formation of the edge temperature pedestal together with the increase in the plasma density and the resultant increase in the heat pinch can improve the energy confinement time significantly.

The formation of the steep edge temperature gradient is confirmed by the 1.5D transport simulation code for our heat pinch transport model. Figure 13 shows the temperature profiles for various particle confinement times in high power NBI heating case ( $P_{\text{NBI}}=20\text{MW}$ ). The density profiles are kept constant for both calculations. As is clear from the figure, the temperature pedestal can be formed if the particle confinement time is sufficiently long and the edge plasma density is sufficiently low ( $n_{\text{eb}} = 0.02n_e(0)$  is assumed for both cases). In the low particle confinement time case, the edge plasma

$$\begin{aligned}\chi_e^{\text{inc}} &= \chi_i^{\text{inc}} = 5 \text{ m}^2/\text{sec} \text{ (uniform)} \\ \tau_p &= 40 \text{ msec} , \sigma = \sigma^{\text{NC}} , Z_{\text{eff}} = 1.0 \\ \bar{n}_e &= 4 \times 10^{19} \text{ m}^{-3} , \text{ multi-pencil beam+Stix solution.}\end{aligned}$$

The agreement with the experimental results is fairly good.

### 3. FORMATION OF THE EDGE TRANSPORT BARRIER IN THE H-MODE

The formation of the edge transport barrier is the most important characteristics of the H mode [12]. The formation of the edge pedestal is associated with the improvement in the particle confinement at the plasma edge which reduces the convective energy loss near the plasma surface [13]. The temperature gradient in our model without the edge convective loss is given by,

$$\frac{dT(r)}{dr} = - \frac{q_{\text{in}} + q_{\text{h}}}{n_e \chi_{\text{inc}}} \quad (30)$$

where,  $q_{\text{h}} = Q_{\text{h}}/S(r)$  is the external heating flux. If the  $\chi_{\text{inc}}$  is finite at the plasma edge, the denominator in the right hand side of the equation (30) becomes zero at the plasma surface. Although  $q_{\text{in}}$  is also zero at the plasma surface,  $q_{\text{h}}$  is finite at the plasma surface. Therefore the temperature gradient at the plasma edge can be very large during a high power heating when the particle confinement is sufficiently good. The formation of the steep temperature gradient at the plasma edge depends strongly on the edge plasma density. For sufficiently low edge plasma density, a steep temperature gradient can be formed. The formation of the edge temperature pedestal together with the increase in the plasma density and the resultant increase in the heat pinch can improve the energy confinement time significantly.

The formation of the steep edge temperature gradient is confirmed by the 1.5D transport simulation code for our heat pinch transport model. Figure 13 shows the temperature profiles for various particle confinement times in high power NBI heating case ( $P_{\text{NBI}}=20\text{MW}$ ). The density profiles are kept constant for both calculations. As is clear from the figure, the temperature pedestal can be formed if the particle confinement time is sufficiently long and the edge plasma density is sufficiently low ( $n_{\text{eb}} = 0.02n_e(0)$  is assumed for both cases). In the low particle confinement time case, the edge plasma

density increases and the temperature gradient expected from the equation (30) becomes small at the plasma edge. Thus the difference in the formation of the edge temperature pedestal will be more enhanced between high  $\tau_p$  and low  $\tau_p$  cases. Experimental observation of the H mode shows that the steep temperature gradient is not formed when the increase of the edge plasma density is very strong during the H mode. This is consistent with our transport model. The formation of the edge transport barrier is the natural consequence of our model from the difference in the radial profiles of the heat pinch and the external heat flux in the case of the good particle confinement at the plasma edge.

#### 4.DISCUSSION AND CONCLUSION

The energy confinement properties of the ohmic and the NB heated plasmas in JT-60 are analyzed based on the empirical heat pinch theory proposed by Callen and Cordey. It is found that the heat pinch flux  $q_{in}$  proportional to  $n_e B_p$  and the constant  $\chi_e^{inc}$  reproduce the ohmic and neutral beam heating results. This transport model is consistent with the temperature profile resilience during the L mode. The model temperature profile is consistent with the experimental profile resilience against the density profile variation. The model is also checked with the 1.5 D transport simulation code. The model predicts the formation of the steep edge temperature gradient when the particle confinement time is sufficiently high. Thus the heat pinch model proposed in this paper can reproduce basic transport characteristics observed during the high power heating in tokamaks. In our transport simulation, we have assumed that both electron and ion have strong heat pinch. But the preliminary investigation of the ion temperature profile by the charge-exchange-recombination spectroscopy shows that the ion temperature profile does not follow profile consistency. Thus the heat pinch term included only in the electron energy balance equation will give better description of the transport properties of the tokamaks. Further study on the subject will be continued in the JT-60U experiment [14].

#### ACKNOWLEDGEMENTS

The authors would like to express their appreciations to Dr. M. Nagami for stimulated discussion on the heat pinch model. The authors would like to express their appreciations to Drs. Y. Shimomura, S. Tamura, M. Tanaka and M. Yoshikawa for continued encouragement and support.



density increases and the temperature gradient expected from the equation (30) becomes small at the plasma edge. Thus the difference in the formation of the edge temperature pedestal will be more enhanced between high  $\tau_p$  and low  $\tau_p$  cases. Experimental observation of the H mode shows that the steep temperature gradient is not formed when the increase of the edge plasma density is very strong during the H mode. This is consistent with our transport model. The formation of the edge transport barrier is the natural consequence of our model from the difference in the radial profiles of the heat pinch and the external heat flux in the case of the good particle confinement at the plasma edge.

#### 4. DISCUSSION AND CONCLUSION

The energy confinement properties of the ohmic and the NB heated plasmas in JT-60 are analyzed based on the empirical heat pinch theory proposed by Callen and Cordey. It is found that the heat pinch flux  $q_{in}$  proportional to  $n_e B_p$  and the constant  $\chi_e^{inc}$  reproduce the ohmic and neutral beam heating results. This transport model is consistent with the temperature profile resilience during the L mode. The model temperature profile is consistent with the experimental profile resilience against the density profile variation. The model is also checked with the 1.5 D transport simulation code. The model predicts the formation of the steep edge temperature gradient when the particle confinement time is sufficiently high. Thus the heat pinch model proposed in this paper can reproduce basic transport characteristics observed during the high power heating in tokamaks. In our transport simulation, we have assumed that both electron and ion have strong heat pinch. But the preliminary investigation of the ion temperature profile by the charge-exchange-recombination spectroscopy shows that the ion temperature profile does not follow profile consistency. Thus the heat pinch term included only in the electron energy balance equation will give better description of the transport properties of the tokamaks. Further study on the subject will be continued in the JT-60U experiment [14].

#### ACKNOWLEDGEMENTS

The authors would like to express their appreciations to Dr. M. Nagami for stimulated discussion on the heat pinch model. The authors would like to express their appreciations to Drs. Y. Shimomura, S. Tamura, M. Tanaka and M. Yoshikawa for continued encouragement and support.

density increases and the temperature gradient expected from the equation (30) becomes small at the plasma edge. Thus the difference in the formation of the edge temperature pedestal will be more enhanced between high  $\tau_p$  and low  $\tau_p$  cases. Experimental observation of the H mode shows that the steep temperature gradient is not formed when the increase of the edge plasma density is very strong during the H mode. This is consistent with our transport model. The formation of the edge transport barrier is the natural consequence of our model from the difference in the radial profiles of the heat pinch and the external heat flux in the case of the good particle confinement at the plasma edge.

#### 4. DISCUSSION AND CONCLUSION

The energy confinement properties of the ohmic and the NB heated plasmas in JT-60 are analyzed based on the empirical heat pinch theory proposed by Callen and Cordey. It is found that the heat pinch flux  $q_{in}$  proportional to  $n_e B_p$  and the constant  $\chi_e^{inc}$  reproduce the ohmic and neutral beam heating results. This transport model is consistent with the temperature profile resilience during the L mode. The model temperature profile is consistent with the experimental profile resilience against the density profile variation. The model is also checked with the 1.5 D transport simulation code. The model predicts the formation of the steep edge temperature gradient when the particle confinement time is sufficiently high. Thus the heat pinch model proposed in this paper can reproduce basic transport characteristics observed during the high power heating in tokamaks. In our transport simulation, we have assumed that both electron and ion have strong heat pinch. But the preliminary investigation of the ion temperature profile by the charge-exchange-recombination spectroscopy shows that the ion temperature profile does not follow profile consistency. Thus the heat pinch term included only in the electron energy balance equation will give better description of the transport properties of the tokamaks. Further study on the subject will be continued in the JT-60U experiment [14].

#### ACKNOWLEDGEMENTS

The authors would like to express their appreciations to Dr. M. Nagami for stimulated discussion on the heat pinch model. The authors would like to express their appreciations to Drs. Y. Shimomura, S. Tamura, M. Tanaka and M. Yoshikawa for continued encouragement and support.

## REFERENCES

- [1] CALLEN, J.D., CHRISTIANSEN, J.P., CORDEY, J.G., THOMAS, P.R., THOMSEN, K., *Nuclear Fusion* 27 (1987) 1857.
- [2] CORDEY, J.G., BARTLETT, D.V., BHATNAGAR, V., BICKERTON, R.J., BURES, M., et al., in *Plasma Physics and Controlled Nuclear Fusion Research 1986* (Proc. 11th Int. Conf. Kyoto, 1986), Vol.1, IAEA, Vienna (1987) 99.
- [3] FREDRICKSON, E.D., CALLEN, J.D., McGUIRE, K, BELL, J., COLCHIN, D., et al., *Nuclear Fusion* 26 (1986) 849.
- [4] TUBBING, B.J.D., LOPES CARDOZO, N.J., VAN DER WIEL, M.J., *Nuclear Fusion* 27 (1987) 1843.
- [5] GOLDSTON, R.J., in *Fifth Tripartite Workshop on Data and Analysis Techniques, "The Physics of Enhanced Confinement Regimes"*, Nice, 1988.
- [6] KIKUCHI, M., HIRAYAMA, T., SHIMIZU, K., et al., *Nuclear Fusion* 27 (1987) 1239.
- [7] SHIMOMURA, Y., ODAJIMA, K., *Comments on Plasma Physics and Controlled Fusion* 10 (1987) 207.
- [8] HINTON, F.L., HAZELTINE, R.D., *Rev. Mod. Phys.* 48 (1976) 239.
- [9] KIKUCHI, M., AZUMI, M., TANI, K. and KUBO, H., submitted to *Nuclear Fusion*.
- [10] STEVENS, J.E., BELL, R., BERNABEI, S., CAVALLO, A., et al., *Nuclear Fusion* 28 (1988) 217.
- [11] SHIMIZU, K., AZUMI, M. et al., to be published.
- [12] WAGNER, F., BECKER, G., BEHRINGER, K., CAMPBELL, D., EBERHAGEN, A., et al., *Phys. Rev. Lett.* 49 (1982) 1408.
- [13] NAGAMI, M., KASAI, M., KITSUNEZAKI, A., KOBAYASHI, T., KONOSHIMA, S., et al., *Nuclear Fusion* 24 (1984) 183.
- [14] KIKUCHI, M., ANDO, T., ARAKI, M., et al, "JT-60 Upgrade Program", 15-th Symp. Fusion Tech. (Utrecht, 1988), paper A05.

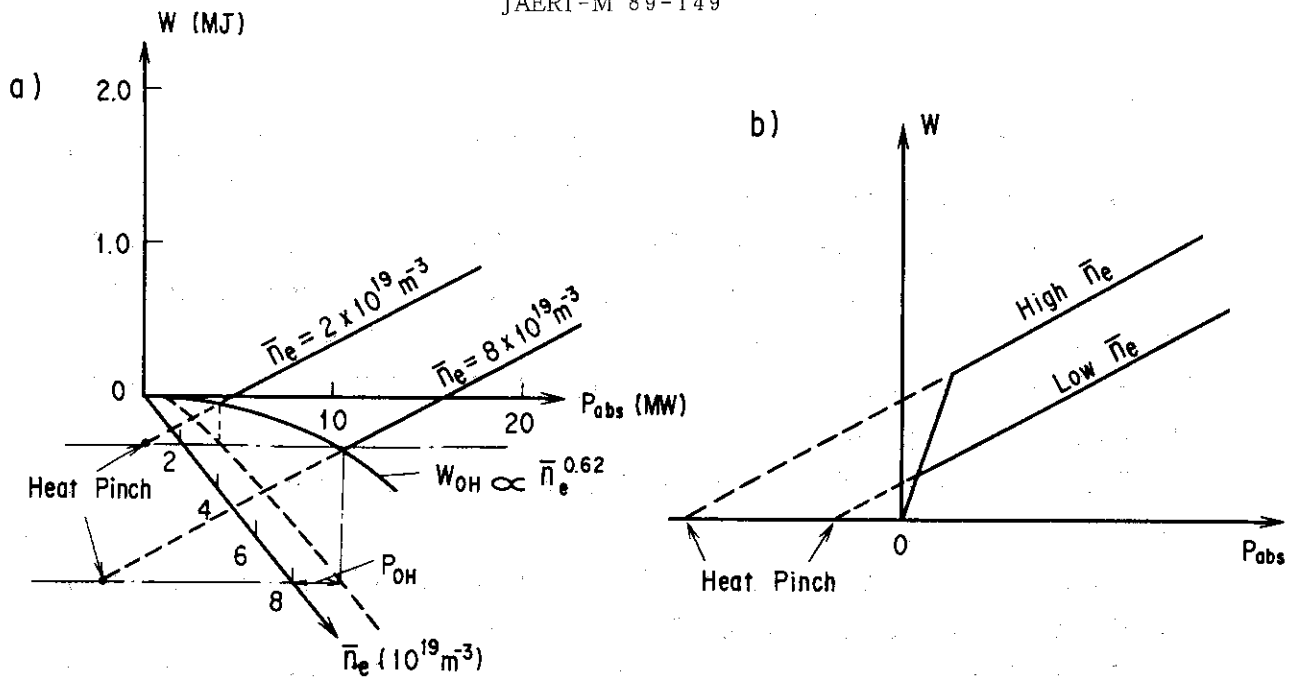


Fig.1 Schematic diagram of the plasma stored energy as a function of  $n_e$  and  $P_{abs}$ . 1a) 3 dimensional plot of the plasma stored energy as a function of  $n_e$  and  $P_{abs}$ . 1b) Offset linear relations of the plasma stored energy for low and high density cases.

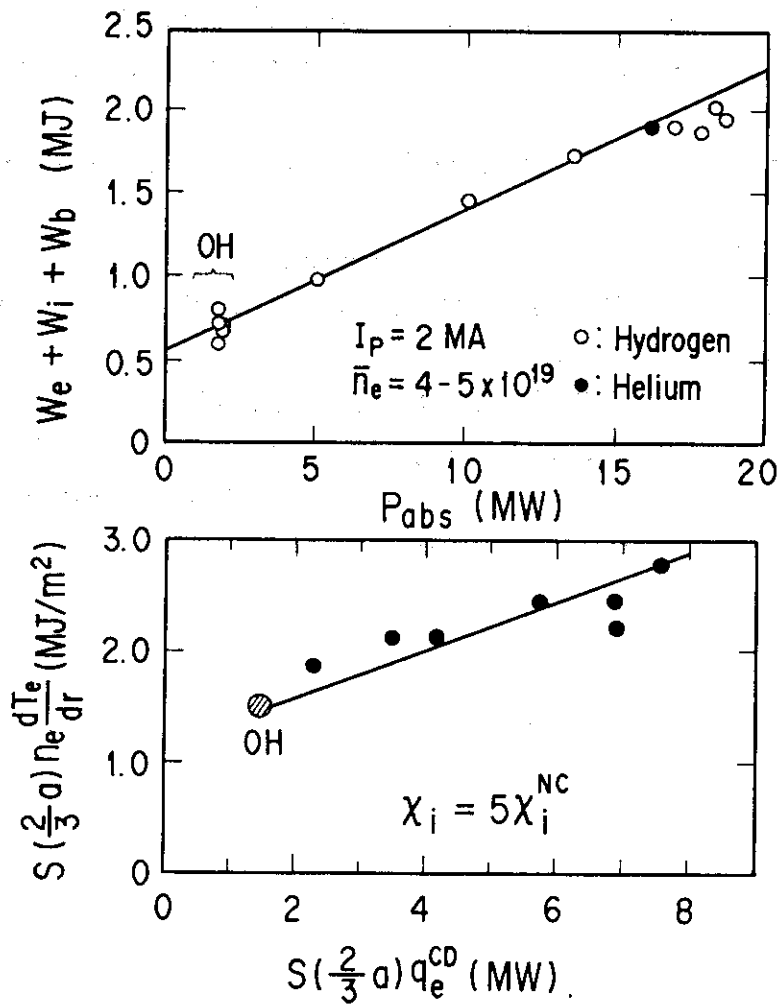


Fig.2 Offset linear relations for the plasma stored energy and the local heat flow at  $r = 2a/3$ .

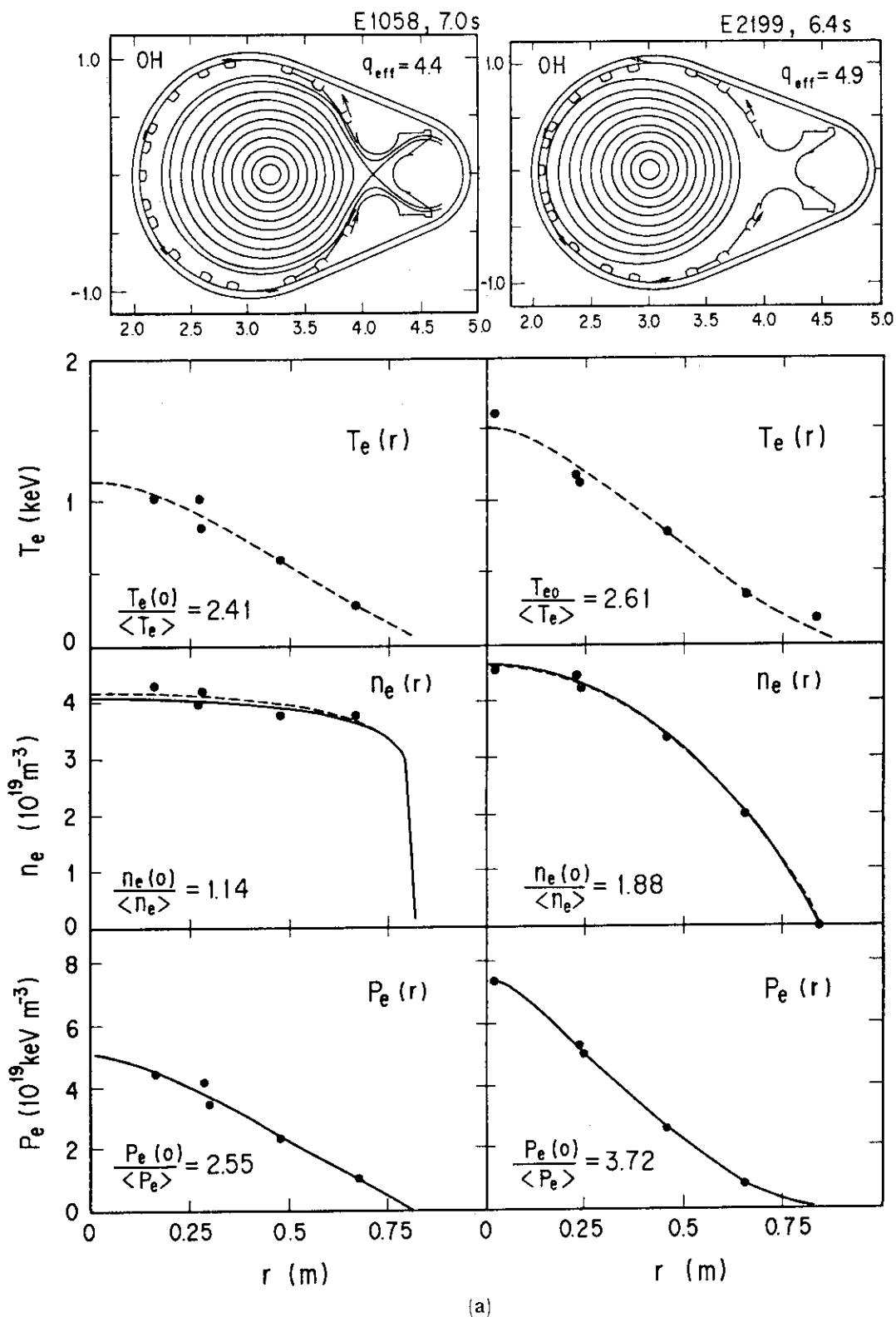


Fig.3 Equilibrium and profile characteristics of ohmic and beam heated discharges.

3a) Profile characteristics of limiter and divertor plasmas in ohmic discharges. Temperature profile does not change while a significant difference in the density profile is observed. As is clear from the figure, the pressure does not exhibit profile consistency. 3b) Profile characteristics of divertor discharges. The temperature profile is insensitive to the density profile peakedness during the beam heating cases.

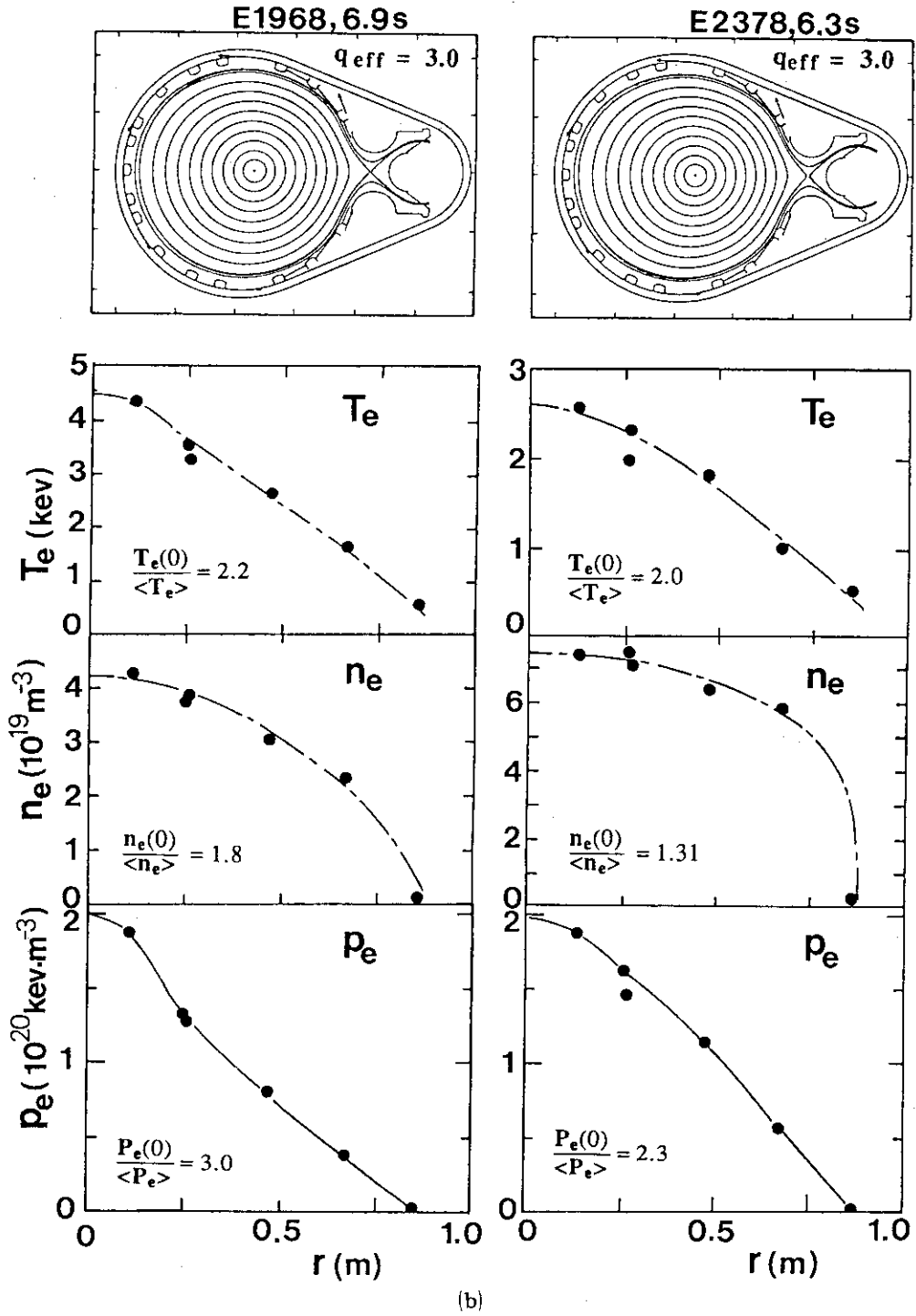


Fig.3 (continued)

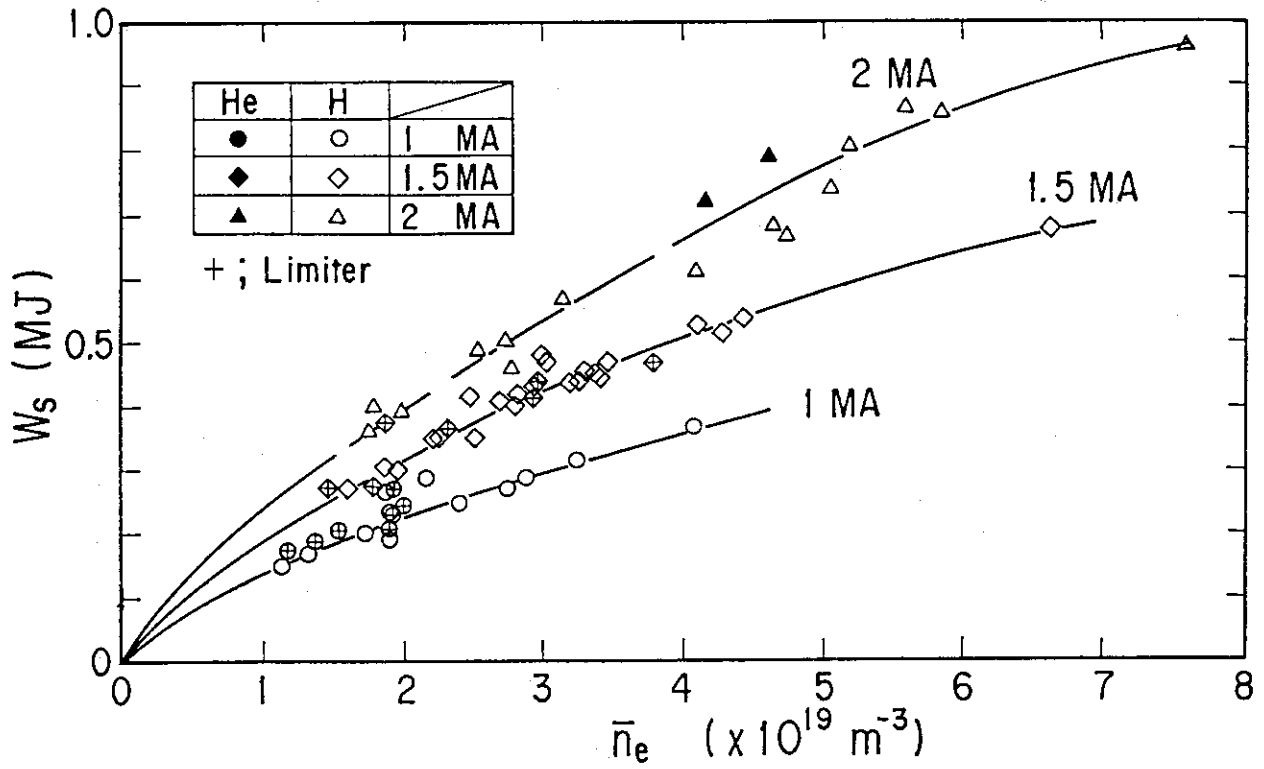


Fig.4 Ohmic plasma stored energy as a function of the line average plasma density for various plasma current evaluated from the Thomson scattering and scoop analysis.

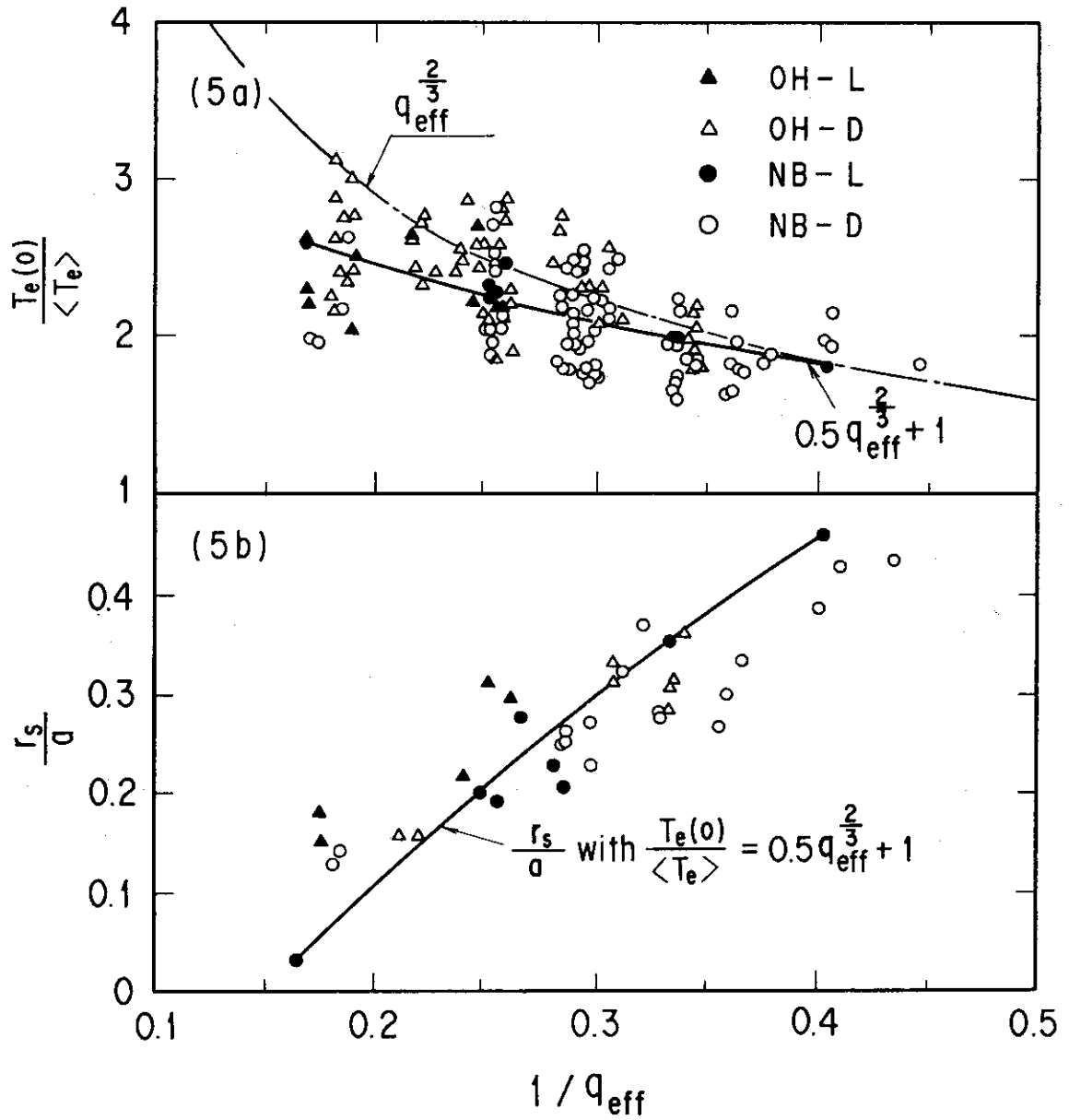


Fig.5 a) The electron temperature profile peakedness parameter as a function of the safety factor  $q_{\text{eff}}$ . b) Radius of the  $q=1$  surface measured by the sawtooth inversion radius. Solid line shows the calculated  $q=1$  radius with the trapped electron correction to the resistivity.



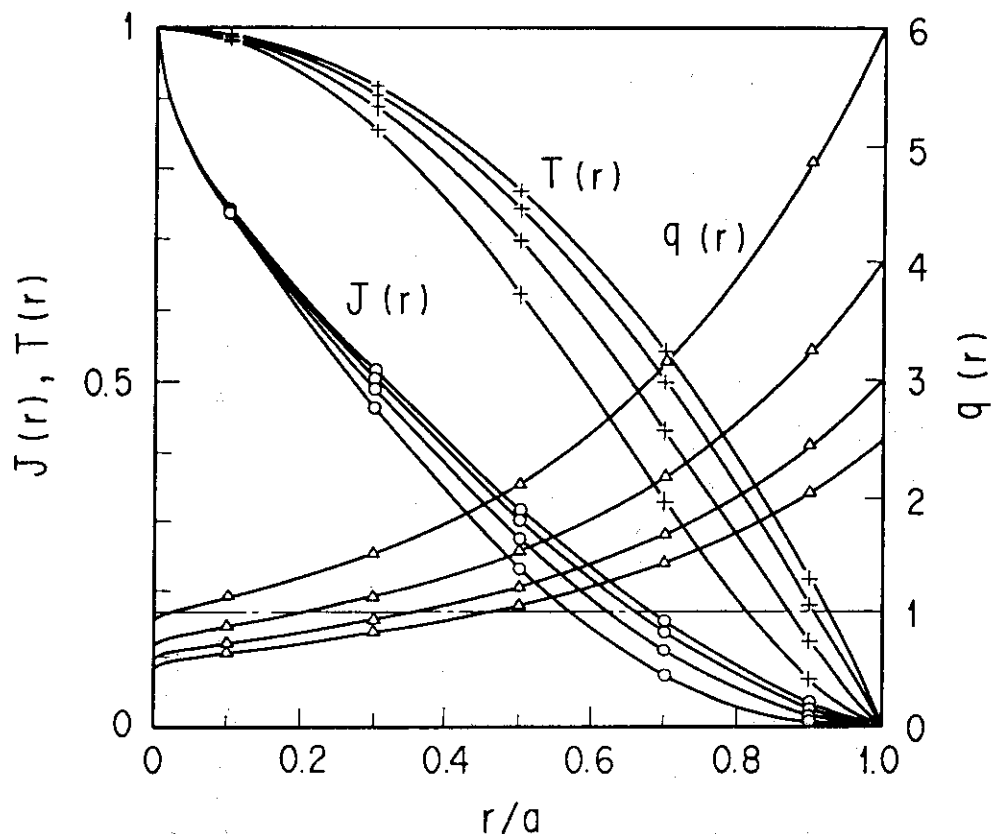


Fig.6 Temperature, current density and safety factor profiles using equations (12) and (13).

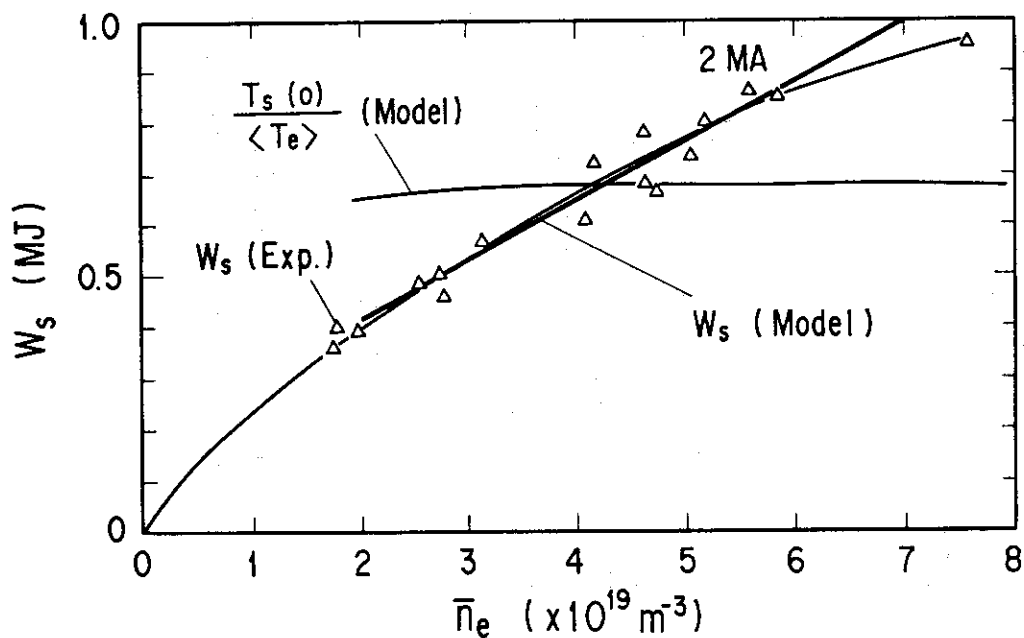


Fig.7 Measured and calculated plasma stored energy as a function of the average plasma density together with the temperature peakedness parameter showing the good reproduction of the ohmic confinement with our model.

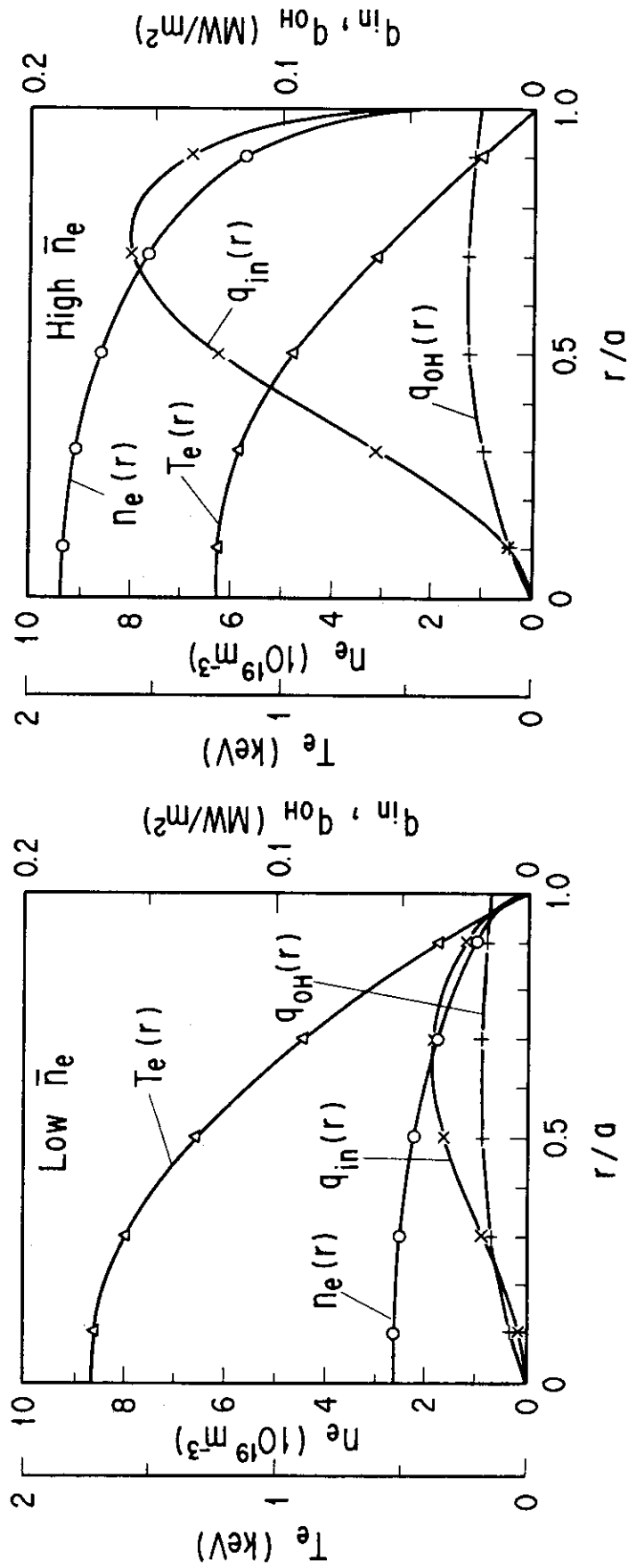


Fig.8 Radial profiles of  $T_e$ ,  $n_e$ ,  $q_{OH}$  and  $q_{in}$  for low and high density ohmic discharges showing the importance of the heat pinch in the ohmic confinement.

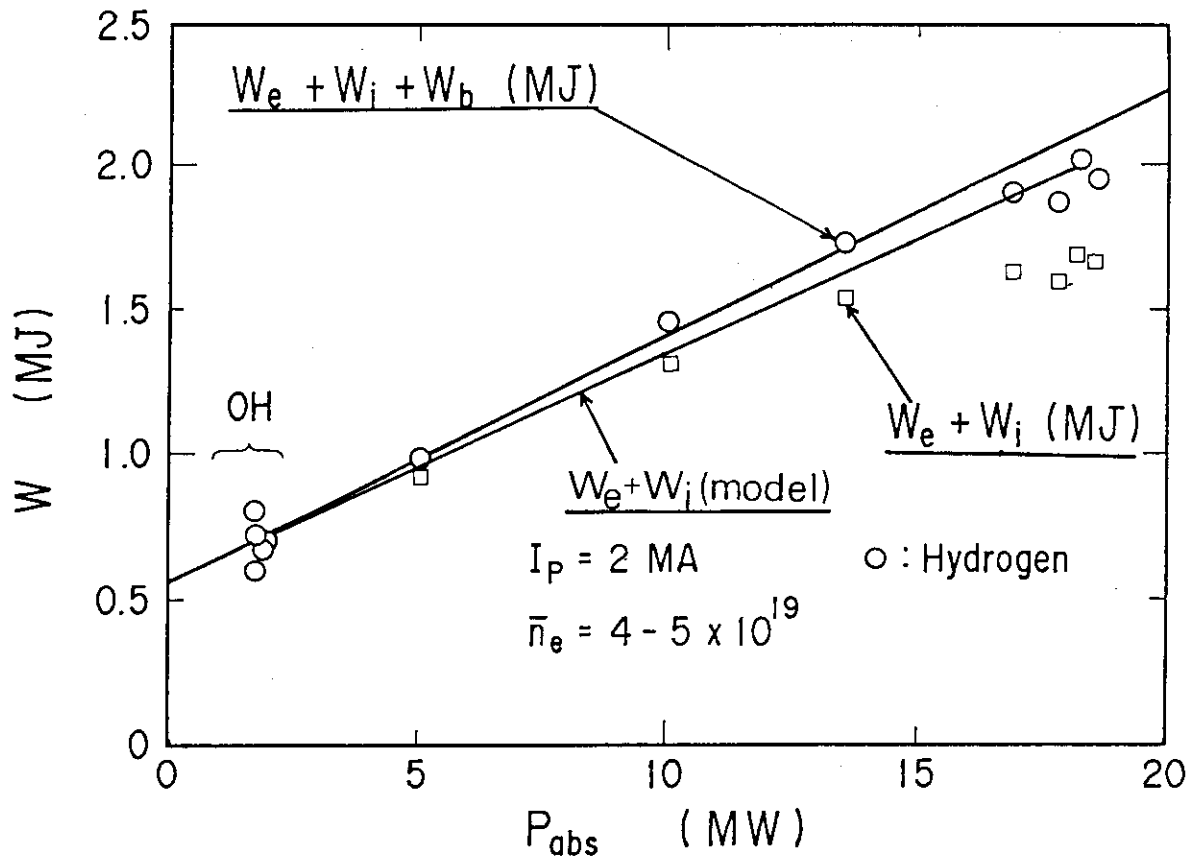


Fig.9 Comparison of the measured and predicted plasma stored energies as a function of  $P_{abs}$  showing the good reproduction of the experimental results with our model.

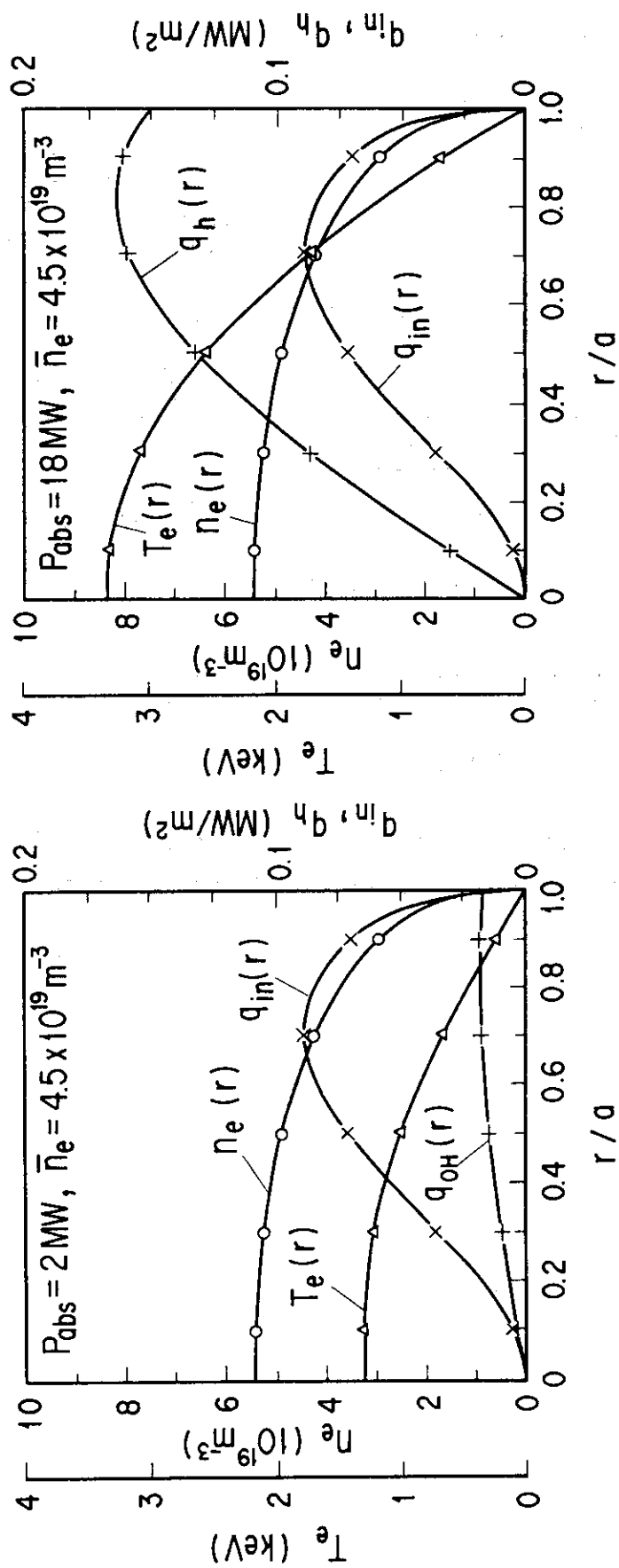


Fig.10 Radial profiles of  $T_e$ ,  $n_e$ ,  $q_h$  and  $q_{in}$  for low and high power NBI heating.

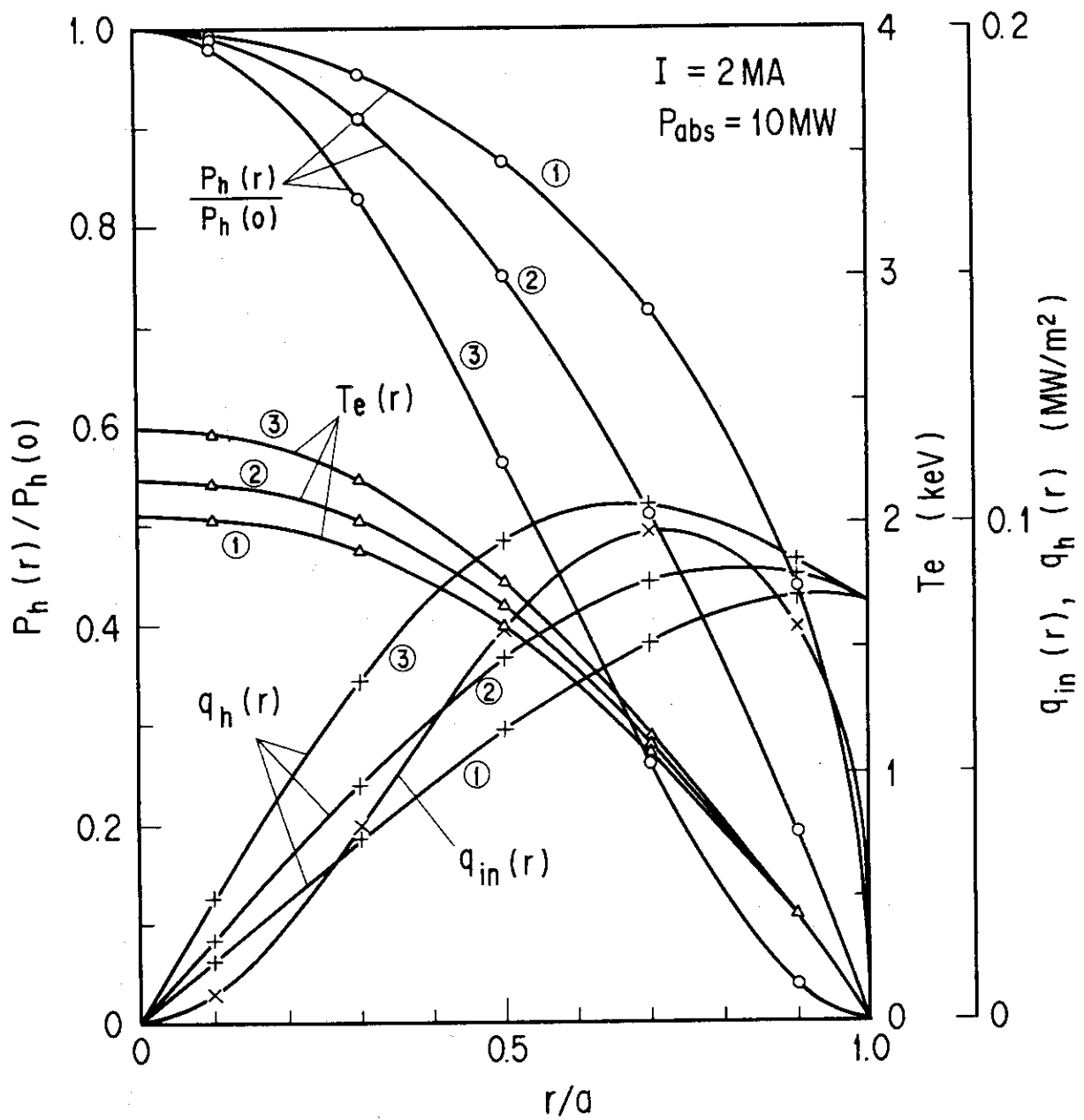


Fig.11 The  $T_e$  profile response to various heating profiles for our heat pinch model.

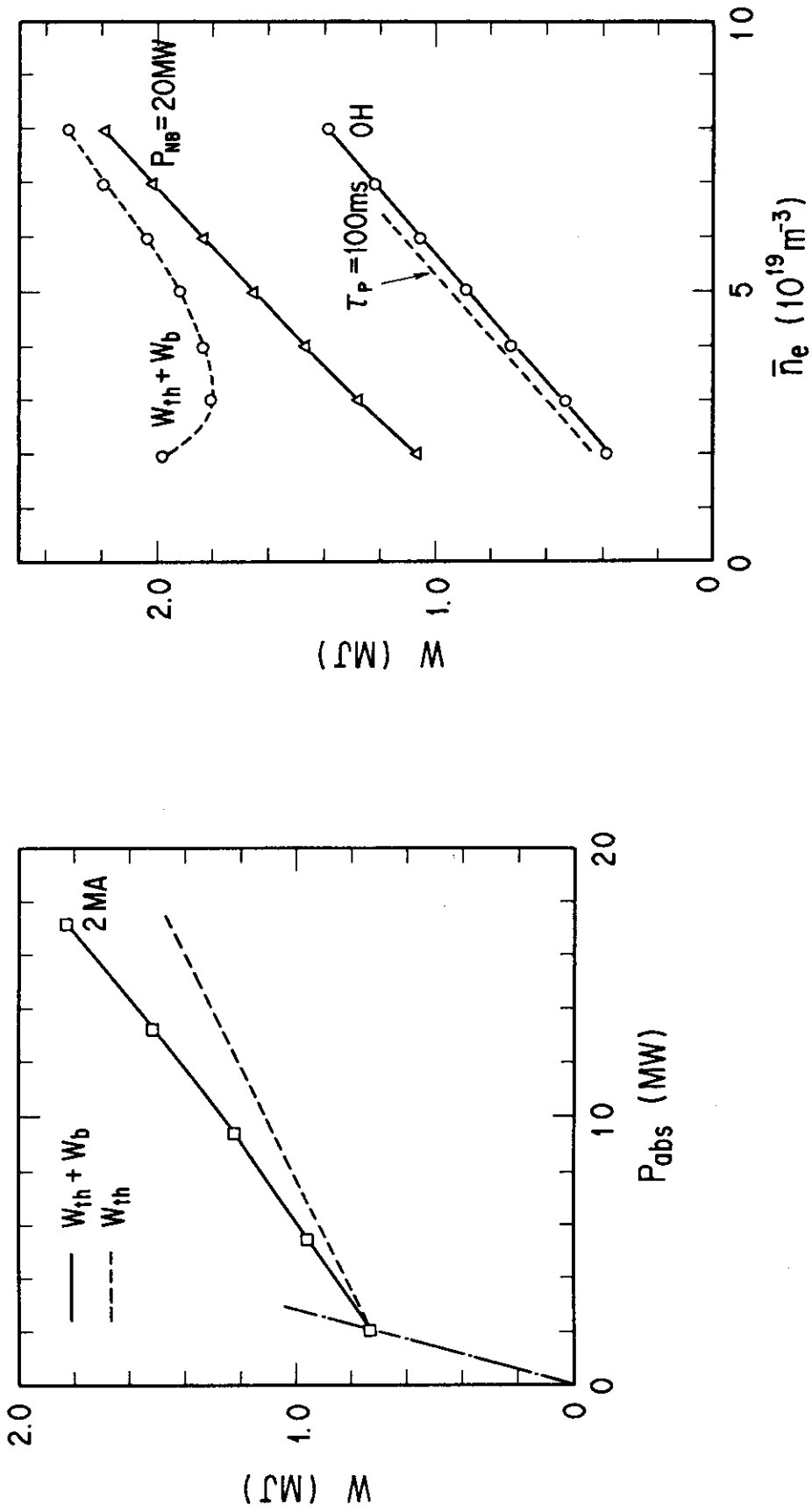


Fig.12 1.5-D transport simulation results of the power and density scan using our heat pinch model. Thermal and beam stored energies ( $W_{th}$  and  $W_b$ ) are shown in the figure.

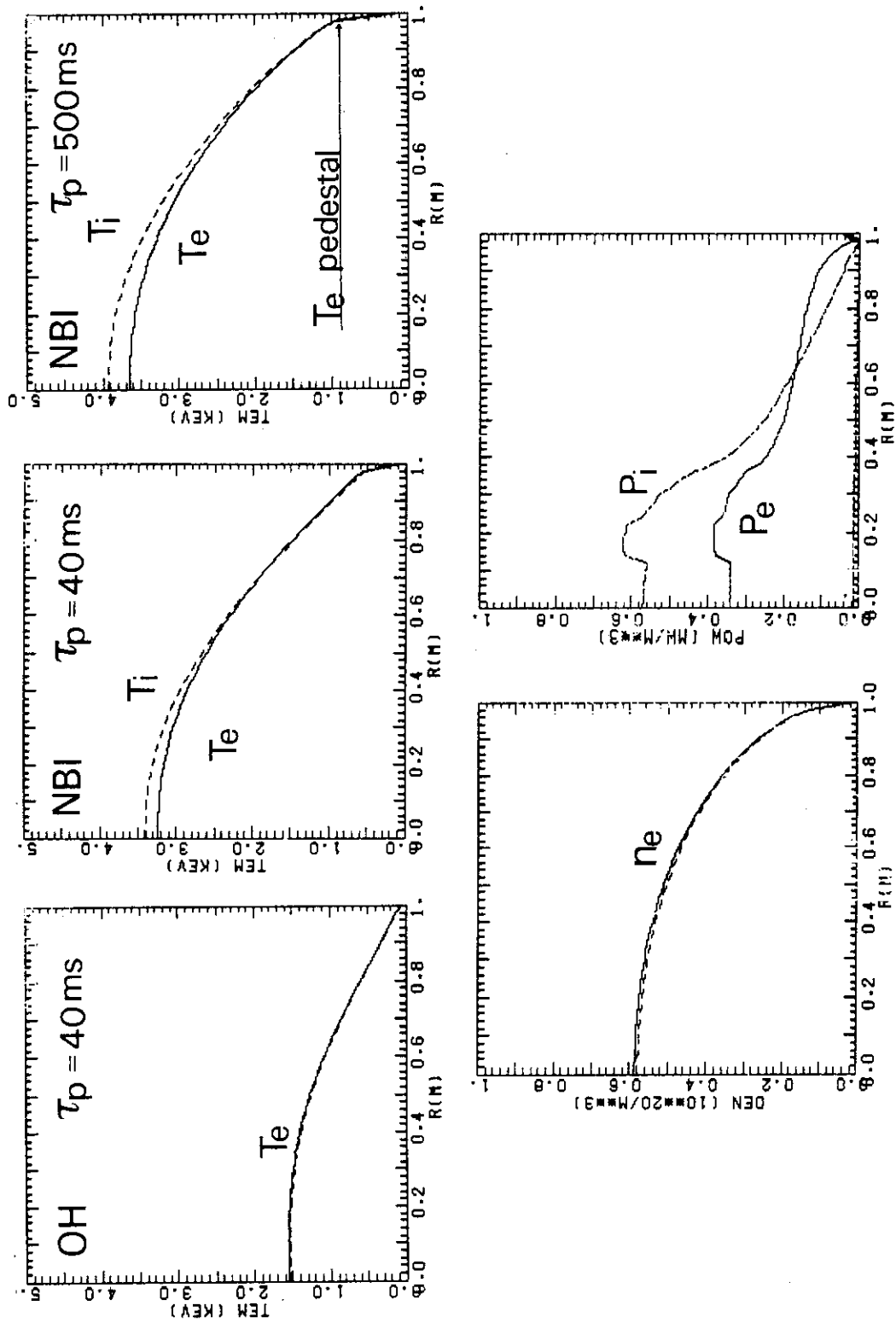


Fig.13 Temperature profiles for ohmic and beam heated discharges ( $P_{NBI} = 20MW$ ). A steep edge temperature pedestal can be seen during the high power heating especially when the particle confinement time is long.